

Signature splitting in nuclear rotational bands: Neutron $i_{13/2}$ systematics

W. F. Mueller, H. J. Jensen,* W. Reviol, L. L. Riedinger, C.-H. Yu,† and J.-Y. Zhang
Department of Physics and Astronomy, University of Tennessee, Knoxville, Tennessee 37996

W. Nazarewicz‡

*Joint Institute for Heavy-Ion Research, Oak Ridge, Tennessee 37831,
 Department of Physics and Astronomy, University of Tennessee, Knoxville, Tennessee 37996,
 and Physics Division, Oak Ridge National Laboratory, Oak Ridge, Tennessee 37831*

R. Wyss

Manne Siegbahn Institute, S-10405 Stockholm, Sweden

(Received 19 October 1993; revised manuscript received 20 June 1994)

Experimental values of signature splitting in $\nu i_{13/2}$ rotational bands in odd- N even- Z nuclei in the $Z = 62-78$ region are collected and presented. A procedure is introduced to calculate signature splitting within the cranked deformed Woods-Saxon model. In the theoretical treatment, deformation parameters are obtained by minimizing the total Routhians of individual $\nu i_{13/2}$ bands, and the procedure accounts for the possibility that the two signatures have different deformations and pairing gaps. Experimental signature splitting data for $\nu i_{13/2}$ bands in Dy, Er, Yb, Hf, W, and Os nuclei are compared with calculated values. The sensitivity of calculated signature splitting to changes in deformation, pairing, and other model parameters is presented.

PACS number(s): 21.10.Re, 21.60.Ev

I. INTRODUCTION

As experiments on high-spin states in nuclei become more sophisticated, a larger quantity of data on the behavior of nuclei at high angular momentum becomes available. This evolution helps to extend the known level schemes both to higher spins and also to more observed rotational bands. The classification of observed bands and their association with available single-particle configurations are always challenges, especially at the limits of experimental detection where information on all of the quantum numbers of a state or a band is very difficult to obtain. In this paper we stress the importance of energy signature splitting in rotational bands, that is the shift between the energetically favored and the unfavored sequences of levels. For the heavier part of the deformed rare earth region, we analyze the trend of signature splitting as a function of proton and neutron number, and we concentrate in the discussion on the neutron systems which are dominated by the $i_{13/2}$ orbital. The discus-

sion includes detailed theoretical calculations of signature splitting. A similar analysis and discussion will be presented at a later time for the proton $h_{9/2}$ orbital.

For a specific analysis of the $\nu i_{13/2}$ signature splitting, it is reasonable to select the nuclei with odd- N and even- Z . Throughout the considered $Z = 62 - 78$ region, the yrast band is built on the neutron $i_{13/2}$ orbital. At low values of rotational frequency, ω , the neutron Fermi level is near the $\Omega = \frac{1}{2}$ substate of the $\nu i_{13/2}$ shell for $N \approx 89, 91$ and so the magnitude of signature-splitting energy is large. The splitting decreases as N increases, but does not reach zero even at $N = 107$ where the $\Omega = \frac{9}{2}$ orbital approaches the Fermi level. An earlier analysis of the trend of the $\nu i_{13/2}$ splitting in this region was performed by Shastry *et al.* [1] for nuclei with $N = 91$ to 101 and $Z = 68$ to 78. Here we extend this trend in both N and Z .

For the theoretical calculation of signature splitting, we take advantage of the fact that the cranked-shell approach works overall very well in explaining the high-spin features of deformed nuclei. However, it is an open question whether current models can reproduce an experimental quantity as "fine" as signature splitting. The magnitude of signature splitting is expected to be very dependent on several properties such as the nuclear deformation, pairing, and shell filling. This makes it difficult to calculate signature splitting with an accuracy comparable to that determined experimentally. There have been earlier theoretical treatments of signature splitting based on the cranked shell model (CSM), e.g., Shastry *et al.* [1]. However, it is clear [2,3] that not only does the deformation of the nucleus vary significantly with the nature of the quasiparticle orbital on which the rotational

*Permanent address: Niels Bohr Institute for Astronomy, Physics, and Geophysics, University of Copenhagen, DK-2100, Copenhagen, Denmark.

†Permanent address: Nuclear Structure Research Laboratory, University of Rochester, 271 East River Road, Rochester, NY 14627.

‡Permanent address: Institute of Theoretical Physics, Warsaw University, 00-681 Warsaw, Poland; Institute of Physics, Warsaw Institute of Technology, Warsaw, Poland.

band is built, but also the deformation can be different for the two signatures, especially for high- j orbitals like those studied here. This difference was not addressed in Ref. [1]. (An extreme example of the deformation-dependence of signature splitting is discussed in Ref. [4] for the $g_{9/2}$ signature partners in ^{79}Rb .)

Total Routhian Surface (TRS) calculations [5,6] have demonstrated this variation of deformation and led to considerable success in explaining experimental data (see, e.g., Ref. [7]). The calculation of energy signature splitting and the comparison to the experimental trend appears to be one of the best ways to test such shape-dependent predictions to a fine enough detail. In this paper, much care is taken to calculate the signature splitting in a microscopic manner, utilizing the difference in deformation and pairing between the two signatures.

In a future publication, we will present the trend in the signature splitting in bands built on the proton $h_{9/2}$ orbital for nuclei in the same region. The yrast band in odd- A isotopes of Ir and Au is built on the mixed $\pi(h_{9/2} \otimes f_{7/2})$ high- j orbital (commonly labeled as $\frac{1}{2}[541]$ or $h_{9/2}$), and the energy splitting is large. For lower values of Z , the signature splitting increases as the $\pi h_{9/2}$ orbital moves above the Fermi level and becomes more of a pure particle state. The splitting is so large that the unfavored signature is not regularly seen, especially since the $\pi h_{9/2}$ band moves up in excitation energy. Nevertheless, there are a number of cases where both signatures are observed, which allows the possibility to test further our calculations on a situation more complex than that for $\nu i_{13/2}$. In the latter case, $i_{13/2}$ is a unique-parity orbital and thus mixing with other configurations can be discounted, at least in the considered range of deformation and spin. However, in the proton case, the presence of close-lying $h_{11/2}$ orbitals makes it difficult to extract accurate deformation parameters for $h_{9/2}$. Consequently, we choose to demonstrate the success of this technique

first for $\nu i_{13/2}$ signature splitting before proceeding to the more difficult $\pi h_{9/2}$ case.

The characteristic signature splitting of a high- j orbital can be used as a fingerprint in the identification of two-quasiparticle bands, and furthermore as a probe of the deformation-driving characteristics of the other orbital in the coupling. As discussed in our preliminary presentations of the signature-splitting systematics [8–10], the analysis of bands in odd-odd nuclei can benefit from this approach. For example, the $\nu i_{13/2}\pi h_{9/2}$ band can be identified by the characteristic signature splitting of the $\nu i_{13/2}$ orbital. Upon closer examination, we have learned that this characteristic splitting is often decreased significantly in the odd-odd case (compared to the adjacent odd- N even- Z case) for $\nu i_{13/2}$ bands due to the coupling to the deformation-driving $\pi h_{9/2}$ orbital [8–10]. Thus, energy signature splitting could be used as a probe of these deformation-driving effects in odd-odd or even-even nuclei, if theory is able to accurately predict this quantity. The comparison with the odd- A single-quasiparticle trend is clearly important to test before trying to use theory in more complicated couplings.

II. GENERAL CONSIDERATIONS

Signature (α) is the quantum number associated with the rotation operator: $R_x(\pi)\psi = e^{(-i\pi j_x)}\psi = e^{(-i\pi\alpha)}\psi$. A symmetry of the nuclear wave function with respect to $R_x(\pi)$ relates states separated by $\Delta I = 2$. For systems with odd particle number, a signature of $\alpha = \frac{1}{2}$ corresponds to rotational bands with $I = \frac{1}{2}, \frac{5}{2}, \frac{9}{2}, \dots$ and $\alpha = -\frac{1}{2}$ for $I = \frac{3}{2}, \frac{7}{2}, \frac{11}{2}, \dots$. As mentioned in Sec. I, a “splitting” can occur between bands differing only in signature. An example of such a splitting in a $\nu i_{13/2}$ rotational band is given in the left portion of Fig. 1 for ^{155}Dy . The rotational sequence on the left

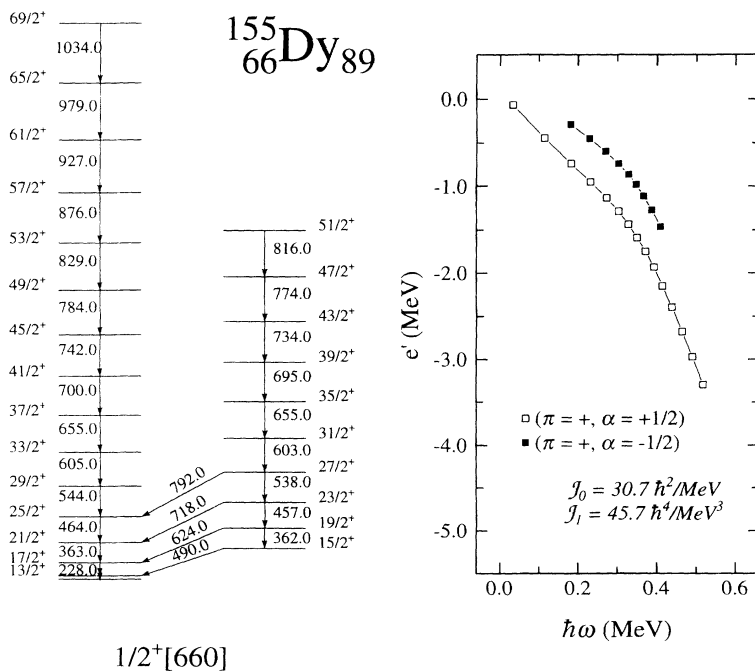


FIG. 1. Level scheme for $\nu i_{13/2}$ band in ^{155}Dy [29]. On the right are the experimental Routhians for the two signatures of this band, with a rotating reference subtracted using the Harris formula and the J_0 and J_1 values shown.

(right) has $\alpha = +\frac{1}{2}$ ($\alpha = -\frac{1}{2}$). As evident from Fig. 1, the $\alpha = +\frac{1}{2}$ sequence is favored in energy when compared to the $\alpha = -\frac{1}{2}$ branch. This large amount of energy difference is expected for $N = 89$ nuclei, where the neutron Fermi level lies in the vicinity of the $\Omega = \frac{1}{2} i_{13/2}$ orbital.

To extract an experimental signature splitting ($\Delta e'$), an observed rotational band is transformed from the laboratory frame to the rotating frame of the nucleus [11]. This is done by calculating the Routhian of the rotational band:

$$E^\omega = E(I) - \hbar\omega I_x, \quad (2.1)$$

where E^ω is the Routhian energy, $E(I)$ is the energy of the level with spin I , $\hbar\omega = \frac{E(I+1) - E(I-1)}{I_x(I+1) - I_x(I-1)}$, $I_x(I) = \sqrt{I(I+1) - K^2}$, and K represents the projection of angular momentum on the nuclear symmetry axis. Then $\Delta e'$ is the difference in energy at a given frequency between the unfavored and favored signatures:

$$\Delta e' = E_u^\omega - E_f^\omega. \quad (2.2)$$

The Routhians for the two signatures of the $\nu i_{13/2}$ bands in ^{155}Dy are shown in the right portion of Fig. 1. The large shift in energy in the unfavored band relative to the favored translates into an energy displacement in the rotating frame. Note that the Routhians shown in Fig. 1 are relative values, after a reference describing the rotational contribution has been subtracted (using the standard Harris parametrization involving J_0 and J_1 values). However, the signature splitting ($\Delta e'$) is independent of this choice of rotating references, since $\Delta e'$ is a difference in Routhian energies at a given ω and the reference energy therefore cancels.

Signature splitting appears within the strong coupling limit of the particle-rotor model as the $2K$ -order correction due to Coriolis perturbation [12]. The corresponding term can be written as

$$\Delta E_I = (-1)^{I+K} \frac{(I+K)!}{(I-K)!} \times (A_{2K} + B_{2K} \hat{I}^2 + C_{2K} \hat{I}^4 + \dots), \quad (2.3)$$

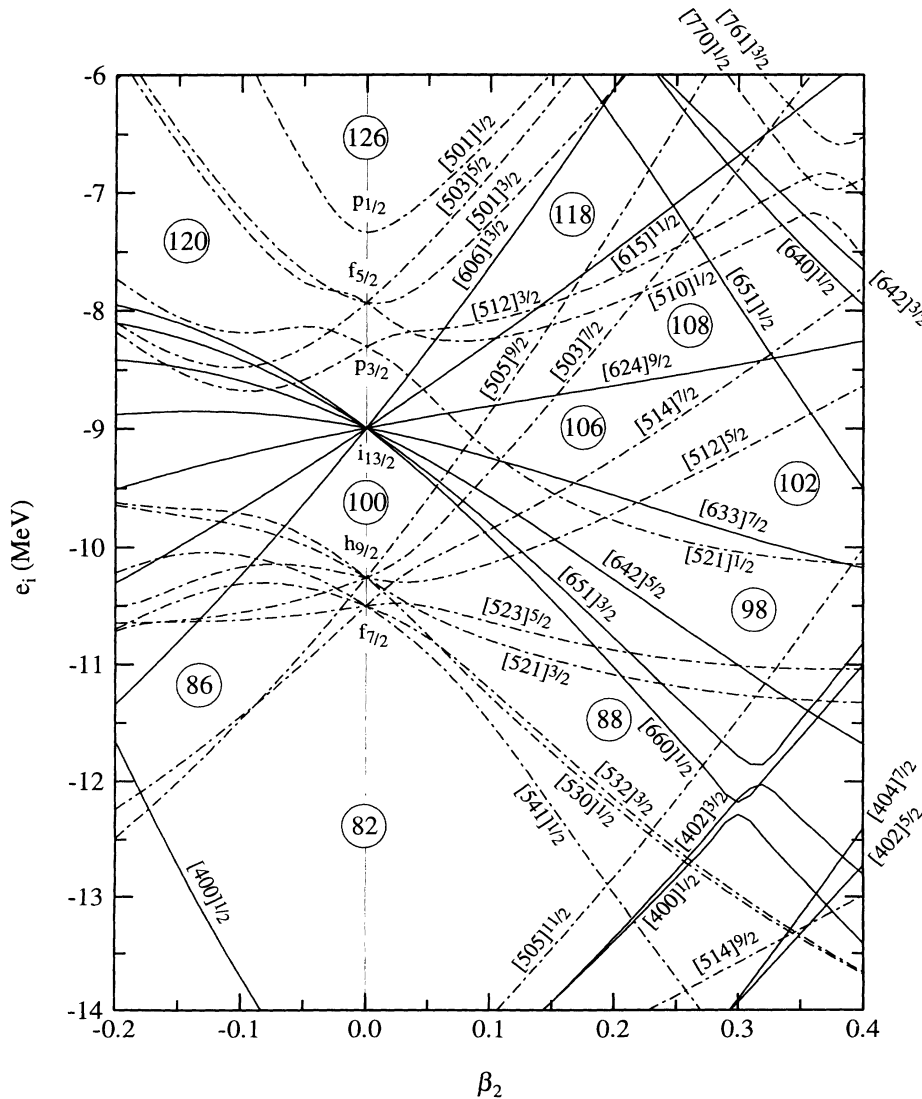


FIG. 2. Single-particle diagram for neutrons using the Woods-Saxon potential as a function of β_2 ($\beta_4 = 0$, $\gamma = 0$).

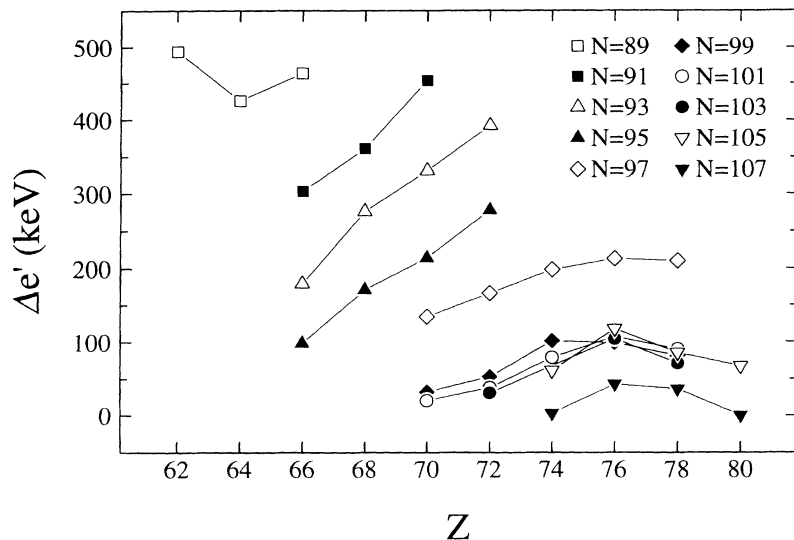


FIG. 3. Experimental signature splitting, at $\hbar\omega = 0.2$ MeV, for the $\nu i_{13/2}$ bands in odd- A , odd- N nuclei. The data for the $N = 89$ isotones (in order of increasing Z) come from Refs. [30,31,29], $N = 91$ from Refs. [32–34], $N = 93$ from Refs. [35–38], $N = 95$ from Refs. [39–42], $N = 97$ from Refs. [43–47], $N = 99$ from Refs. [43,48–51], $N = 101$ from Refs. [52,53,49,54,55], $N = 103$ from Refs. [56,54,57], $N = 105$ from Refs. [58–61], $N = 107$ from Refs. [62,59,63,64].

where $\hat{I} = \sqrt{I(I+1)}$ and the expansion coefficients A, B, C, \dots do not depend on I . A similar perturbative estimate can be carried out in the framework of the cranking model. Here the Coriolis perturbation is represented by the cranking term, $-\hbar\omega I_x$. For a high- j Nilsson orbital, signature splitting appears as the 2Ω -order effect in the ω expansion. To be more specific, for low values of ω , $\Delta e'$ is proportional to ω for $\Omega = \frac{1}{2}$, it behaves as ω^3 for $\Omega = \frac{3}{2}$, and so on. This leads to decreasing signature splitting with the filling of the high- j shell; the Coriolis perturbation becomes weaker with increasing N . An important contribution to $\Delta e'$ comes from shape changes. For example, in the lowest order $\Delta e'$ decreases with quadrupole deformation, β_2 , as $(\beta_2)^{-2\Omega+1}$ if pairing is neglected. In the limit of rotational alignment the signature splitting (for an $\Omega = \frac{1}{2}$ configuration) approaches a maximum value of $\Delta e' = \hbar\omega$, if one neglects the relative variations in the mean field for the signature partners due to deformation and pairing. It is interesting to note that the phenomenon of signature splitting has a classical interpretation in terms of the $C_{2\nu}$ bifurcation caused by the Coriolis force [13].

III. EXPERIMENTAL SYSTEMATICS FOR $\nu i_{13/2}$ BANDS

Bands built on $i_{13/2}$ neutron orbitals are observed in odd- N nuclei with $Z = 62 - 78$. This presents an excellent case for following the systematic trend of signature splitting over a wide range of N and Z values. As seen in the single-particle diagram of Fig. 2, the neutron Fermi levels move from low in the shell (for $N = 89$) to the higher- Ω $\nu i_{13/2}$ orbitals at $N = 107$, the limit of this survey. The $\nu i_{13/2}$ data present a good case for detailed calculations since this is the only positive parity state in the region, and so there is little mixing with other states. The experimental values of signature splitting, $\Delta e'$, are extracted from all known $\nu i_{13/2}$ rotational bands for odd- A nuclei in the rare-earth region and shown in Fig. 3 and

Table I. These $\Delta e'$ values are listed for $\hbar\omega = 0.2$ MeV, which is well below the first band crossing in each case.

The systematic trend of $\nu i_{13/2}$ signature splitting is a smooth and clear function of both the neutron and proton numbers. The signature splitting decreases as the neutron number increases, which is a result of the Fermi level moving to the higher Ω orbitals in the $\nu i_{13/2}$ shell, as discussed above (see Fig. 2). This results in a reduced mixing with the $\frac{1}{2}^+[660]$ configuration, and thus produces a smaller signature splitting. The $\Delta e'$ values smoothly drop for each increasing value of N and thus successively higher values of Ω , at least up until $N = 99$. The similar $\Delta e'$ for $N = 99, 101, 103,$ and 105 is a result of the Fermi level being in a transition region from down-sloping to up-sloping single-particle orbitals. Even for a given value of N , there are large (but smooth) variations in the $\nu i_{13/2}$ signature splitting among the isotones, which is a result of deformation differences. As discussed above, for a given N , a smaller β_2 value leads to increased mixing of the $\nu i_{13/2}$ orbitals of higher Ω with that of $\Omega = \frac{1}{2}$. This increased Ω mixing gives a larger signature splitting for that isotonic chain. To illustrate this correlation, we present in Fig. 4 the calculated [14] quadrupole

TABLE I. Experimental energy signature splitting, $\Delta e'$ (in keV), for the $\nu i_{13/2}$ bands in odd- A , odd- N nuclei. The values are extracted at $\hbar\omega = 0.2$ MeV. For experimental references, see caption to Fig. 3.

	Sm	Gd	Dy	Er	Yb	Hf	W	Os	Pt	Hg
89	494	426	464	—	—	—	—	—	—	—
91	—	—	303	361	454	—	—	—	—	—
93	—	—	179	276	331	392	—	—	—	—
95	—	—	98	171	214	278	—	—	—	—
97	—	—	—	—	134	166	198	213	210	—
99	—	—	—	—	32	53	101	99	81	—
101	—	—	—	—	20	38	79	107	90	—
103	—	—	—	—	—	31	—	104	71	—
105	—	—	—	—	—	—	61	118	85	67
107	—	—	—	—	—	—	3	43	36	0

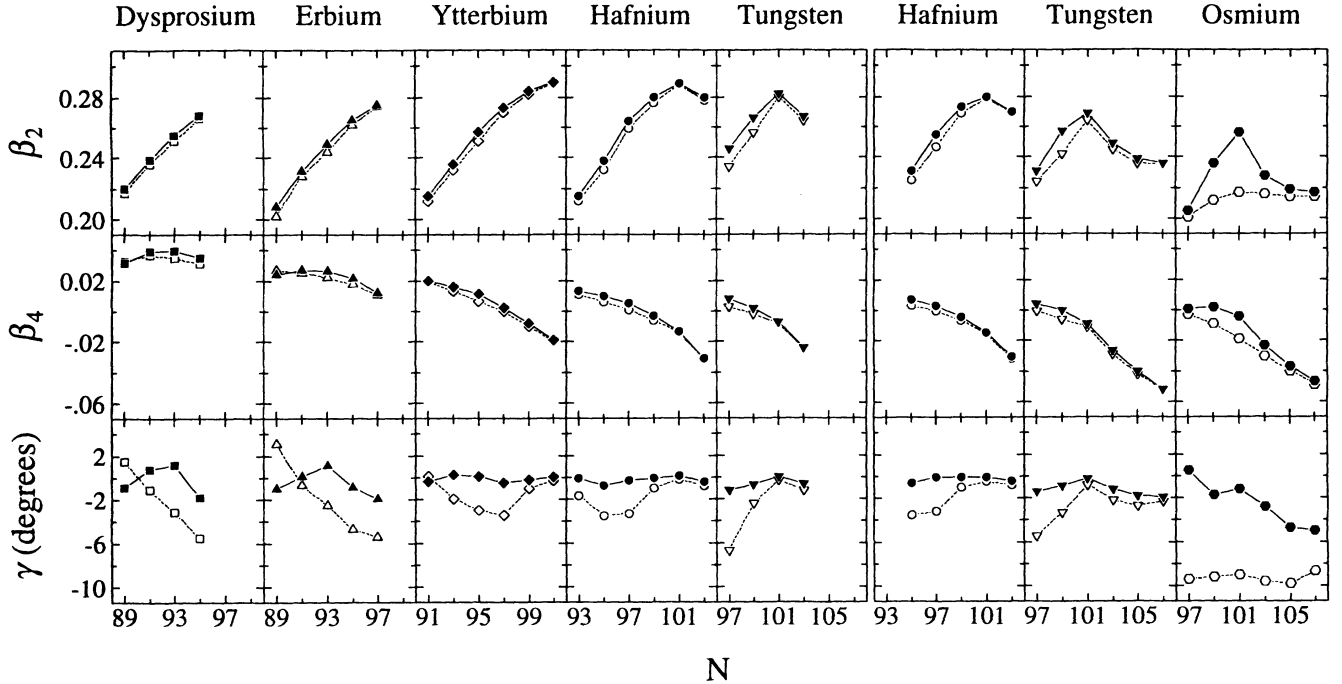


FIG. 4. Deformation parameters at $\hbar\omega = 0.2$ MeV for the $\nu i_{13/2}$ signature partners of odd- N even- Z isotopes of Dy–Os. These values in the left panels were extracted from Yb-mesh TRS calculations, the Hf, W, and Os values in the right panels are from the Pt-mesh TRS calculations. The open symbols refer to the favored signature ($\alpha = \frac{1}{2}$), and the solid symbols to the unfavored signature ($\alpha = -\frac{1}{2}$). See text for description of the Yb and Pt meshes.

deformations for the favored ($\alpha_f = \frac{1}{2}$) and unfavored ($\alpha_f = -\frac{1}{2}$) $\nu i_{13/2}$ orbitals throughout the region. Note from Fig. 4 that the β_2 values in $N = 91$ ($\Omega = \frac{3}{2}$) isotopes, for example, decrease from Dy to Yb, respectively. By comparison, the corresponding experimental $\Delta e'$ for the $\nu i_{13/2}$ bands in these nuclei increase, indicating some relationship between deformation and signature splitting. It is one purpose of the calculations described in the next section to test the exact nature of that relationship.

IV. CALCULATION OF SIGNATURE SPLITTING

The experimental trend of $\nu i_{13/2}$ signature splitting (shown in Fig. 3) is strongly dependent on Fermi level and deformation, as demonstrated in Sec. III. Shastry *et al.* [1] obtained good agreement between the Yb part of their systematic data and CSM calculations. They used deformation parameters (ϵ_2 , ϵ_4 , and γ) extracted from minimized potential energy calculations, and then calculated $\nu i_{13/2}$ signature splitting in a standard CSM approach using average values of the deformation parameters of the two signatures. In this section, we describe calculations which attempt to reproduce a wider set of collected data on $\nu i_{13/2}$ signature splitting. Furthermore, a more detailed theoretical approach is taken here than in Ref. [1], in order to include the fact that at high spins the two signatures of the $\nu i_{13/2}$ band have somewhat different deformation parameters and pairing fields.

As shown in the previous section, signature splitting is obviously dependent on deformation and shell filling. Furthermore, deformation and Fermi level are very interdependent and also functions of pairing as well. Small changes in deformation can alter the single-particle level density near the Fermi level, which clearly affects the pairing energy of the system. Because of this interdependence, the most proper procedure to calculate $\Delta e'$ would be one in which the *total* Routhian energy of a particular state is minimized with respect to deformation parameters and pairing, with the appropriate quasiparticle configuration blocked. Such a microscopic calculation has not been completed at this time, so instead we have developed a procedure that includes self-consistency in separate steps.

Certainly, signature splitting of a rotational band can be extracted from TRS calculations by taking the difference between the calculated total Routhian energies of the unfavored and favored signatures. However, there are clear difficulties associated with this approach. The TRS calculation was developed in order to extract the nuclear deformation (β_2 , β_4 , and γ) as a function of rotational frequency for different quasiparticle configurations, and for this purpose the approach is quite successful. However, our TRS calculations were not optimized for calculating Routhian energies. In the execution of the TRS calculations, neighboring nuclei are organized into groups, referred to as meshes, in this paper. These meshes tend to be limited in the number of nuclei that they contain, because it is not feasible to perform a com-

plete minimization of deformation and energy over a wide range of nuclei. For each mesh, the Woods-Saxon parameters are optimal for the central nucleus of the mesh and are used in the calculation of the single-particle levels for all the nuclei in the mesh. This produces slightly improper single-particle levels and wave functions for the other nuclei, particularly at the edges of the mesh. Another source of uncertainty is that the total Routhian energies are calculated only at prescribed points of a deformation grid, and values at a minimized deformation between the grid points must be interpolated. Furthermore, to simplify calculations, pairing in TRS is treated self-consistently only at $\omega = 0$, and for $\omega > 0$ is varied according to a simple phenomenological formula.

We have developed an approach for calculating signature splitting that uses the features and flexibility of an HFB-based cranking model.¹ In this approach the total signature splitting is decomposed into two components:

$$\Delta e' = \Delta E_{\text{def}} + \Delta E_{\text{rot}}. \quad (4.1)$$

ΔE_{def} is the difference in vacuum (or bandhead) energy resulting from a difference in deformation between the two signature partners, and ΔE_{rot} is the energy difference that results from the different dependence of rotation for the signature partners of a band.

The TRS calculation provides a “realistic” (i.e., frequency-dependent) estimate of deformation for a given rotational structure. Therefore, in our treatment, deformation parameters are extracted from TRS at the rotational frequency, ω_0 , that is of interest for calculating signature splitting, and then are used for the calculations of ΔE_{rot} .

The CSM code used in this analysis is based on the pairing self-consistent cranking model with a Woods-Saxon potential [15]. The deformation parameters from TRS for the favored and unfavored signatures of a high- j configuration are used in separate cranking calculations for the blocked configuration to extract the Routhian energy for each signature. The quantity $\Delta E_{\text{rot}}(\omega_0)$ then is the difference between the change in energy due to rotation at frequency ω_0 for the unfavored signature and that for the favored signature:

$$\Delta E_{\text{rot}} = E_{\text{rot}}^u - E_{\text{rot}}^f = [E^u(\omega_0) - E^u(\omega = 0)] - [E^f(\omega_0) - E^f(\omega = 0)]. \quad (4.2)$$

To obtain the energy difference of the vacua of the two states (ΔE_{def}), we use the Strutinsky renormalization procedure. The difference between the vacuum energies of the unfavored and the favored signature is the energy difference resulting from different nuclear deformations

(ΔE_{def}). The improvement of this new technique over previous methods of calculating signature splitting results from the fact that (a) a self-consistent pairing treatment can be used with the TRS calculated deformation parameters and (b) different deformations and pairing for the two signatures are included.

V. CALCULATED $\nu i_{13/2}$ SIGNATURE SPLITTING

Signature splittings for known $\nu i_{13/2}$ rotational bands in Dy, Er, Yb, Hf, W, and Os isotopes were calculated at $\hbar\omega = 0.2$ MeV using the method introduced in Sec. IV. We do not perform these calculations for the elements at the limits of this experimental survey (Sm, Gd, Pt, and Hg) due to increasing softness toward γ deformation and/or the presence of prolate-oblate coexistence effects. There are two meshes of TRS calculations that contain nuclei in our region of interest. One mesh uses ¹⁶⁸Yb as the central nucleus [14] for which Woods-Saxon parameters are optimized. This mesh contains calculations for nuclei with $Z = 64 - 74$ and $N = 84 - 104$. A second mesh is centralized around ¹⁸²Pt [16], with calculations for nuclei with $Z = 72 - 82$ and $N = 94 - 118$. We refer to these two as the Yb mesh and the Pt mesh, respectively. The deformation parameters at $\hbar\omega = 0.2$ MeV for these nuclei were obtained from these two groups of TRS calculations and are summarized in Fig. 4. For Hf ($Z = 72$), there are experimental data for $N = 93 - 103$, but the Pt mesh does not extend down to ¹⁶⁵Hf ($N = 93$). Likewise, there are experimental data for W ($Z = 74$) with $N = 97 - 107$, but there are no Yb-mesh deformation parameters for W isotopes with $N > 103$. In comparing the deformation parameters from the Yb and Pt meshes for the overlapping nuclei, one finds that the parameters from the Pt mesh are about 5% smaller than those from the Yb mesh. This difference is primarily due to the different size of the central nucleus in each mesh.² Slightly different pairing treatments, and other minor differences between the mesh calculations also contribute to the difference in the deformation parameters.

With the exception of Os, the trend in deformation as a function of neutron number is similar for all the elements studied. There is a steady increase in quadrupole deformation (β_2) with neutron number for each element up to $N = 101$, after which β_2 begins to decrease. For $N > 101$ up-sloping orbitals are being filled (see Fig. 2), which results in a decreased quadrupole deformation. For these cases the deformation variations in the hexadecapole (β_4) and triaxial (γ) degrees of freedom are small in compar-

¹The term HFB (Hartree-Fock-Bogolyubov) should be understood in the sense of the general Bogolyubov transformation which defines quasiparticles at high spins in the presence of a pairing field. The particle-hole mean field is, in our model, not computed self-consistently, but rather approximated by the ω -independent deformed Woods-Saxon potential.

²In the TRS calculations the function that defines the shape of a nucleus depends on the nuclear radius and, hence, on the mass of the central nucleus of the mesh. More specifically, $R \propto A^{\frac{1}{3}}(1 + \sum_{\lambda\mu} \alpha_{\lambda\mu} Y_{\lambda\mu})$. For R to remain the same for a given nucleus, the mesh with the heavier central nucleus will predict a slightly smaller deformation than a mesh with a lighter central nucleus.

TABLE III. Calculated pairing (in keV) for the favored (Δ_f) and unfavored (Δ_u) signatures of the $\nu i_{13/2}$ bands of ^{155}Dy and ^{167}Yb . NSC denotes the pairing result with a non-frequency-dependent pairing treatment, without blocking. SC @ 0 denotes the pairing result from a frequency-dependent self-consistent pairing calculation with blocking at $\hbar\omega = 0$, and SC @ 0.2 is a similar result at $\hbar\omega = 0.2$ MeV. $\delta\Delta$ is defined to be $\Delta_u - \Delta_f$.

	^{155}Dy			^{167}Yb		
	NSC	SC @ 0	SC @ 0.2	NSC	SC @ 0	SC @ 0.2
Δ_f	906	664	544	831	610	395
Δ_u	912	671	639	824	605	514
$\delta\Delta$	6	7	95	-7	-5	119

frequency independent and calculated from BCS theory without blocking at $\hbar\omega = 0$. The ΔE_{rot} calculated using this approximate treatment and the successful calculations of ΔE_{rot} using the pairing-self-consistent treatment are compared in Fig. 5, along with ΔE_{def} . While the pairing treatment is quite different in both calculations of ΔE_{rot} , the results are very similar. This can be understood by looking at the specific examples referred to in Table III. For both ^{155}Dy and ^{167}Yb there is a dramatic difference in pairing energy between the two models due to blocking. Also note that the difference in Δ between the two signatures ($\delta\Delta$) is small at $\hbar\omega = 0$ for both nuclei, but quite large at $\hbar\omega = 0.2$ MeV for the self-consistent pairing treatment. The energy of the band

at $\hbar\omega = 0$ is very sensitive to changes in Δ . However, $\Delta e'$ is a difference between two Routhians, therefore the absolute Δ value is not as important as the relative Δ value between the two signatures, which for both pairing models is quite small at $\hbar\omega = 0$. With increasing $\hbar\omega$, the Coriolis term ($-\omega I_x$) becomes increasingly important, therefore the pairing differences at $\hbar\omega = 0.2$ MeV (and higher frequencies as well) do not have a significant effect on $\Delta e'$ (see discussion below).

Figure 6 shows the comparison between the calculated signature splitting and $\Delta e'$ extracted from experimental data. The calculated $\Delta e'$ [Eq. (4.1)] is obtained using the non-self-consistent pairing treatment. For the nuclei where the Yb and Pt meshes overlap, the calculated $\Delta e'$ using the different deformation parameters from the respective meshes agree well. Also, the calculated $\Delta e'$ values calculated by this method are in good agreement with experiment, except for $N = 101$ W and Os, $N = 99$ Os, and the light Dy nuclei. The calculated signature splitting in these W and Os nuclei is generally too low. Part of this effect can be associated with theoretically overestimated quadrupole deformations around the deformed $N = 102$ gap in the single-particle orbitals (Fig. 2). Indeed, precisely at $N = 100, 102$ the calculated equilibrium values of β_2 for the ground-state configurations of even-even rare-earth nuclei are systematically higher as compared to experimental data, and the deviation strongly increases when going from Yb to Hf (see Table 1 and Fig. 6 in Ref. [18]). The largest deviations between experimental and theoretical signature splitting

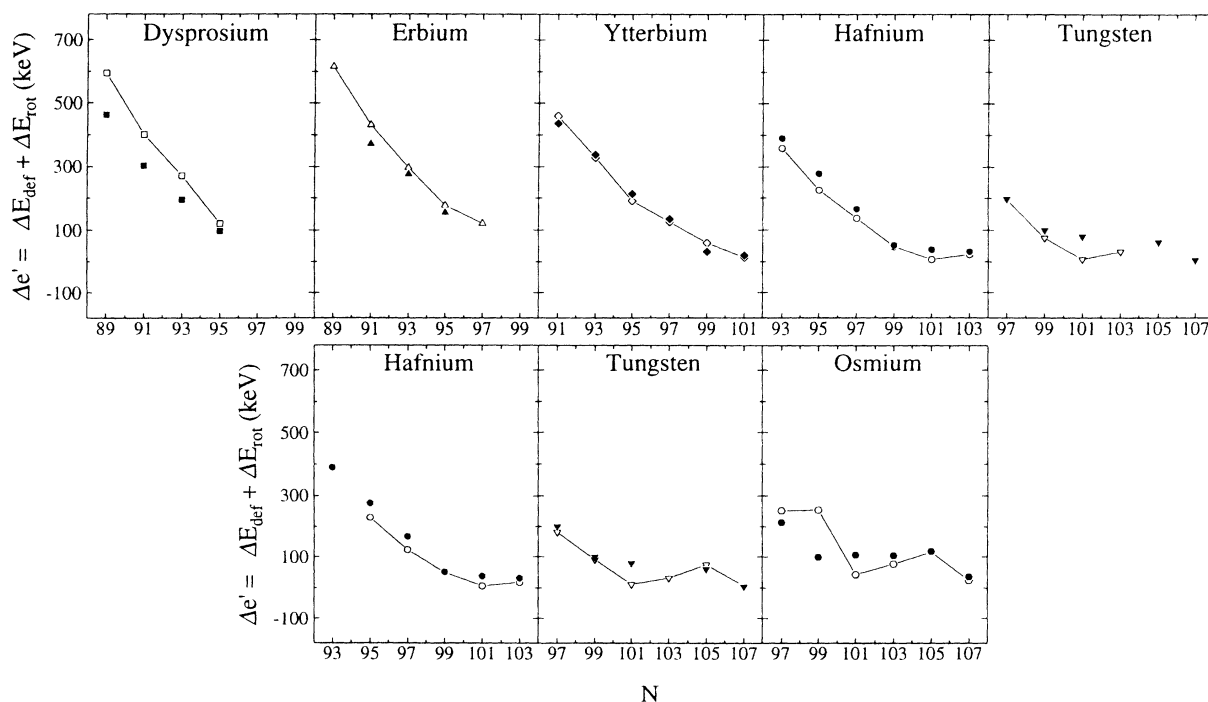


FIG. 6. Experimental and calculated $\nu i_{13/2}$ signature splitting at $\hbar\omega = 0.2$ MeV for isotopes of Dy–Os. The experimental data (labeled by solid symbols) are the same as in Fig. 3, and the calculated values (open symbols) were obtained using the procedure presented in this paper. The upper panels show the calculated $\Delta e'$ using deformation parameters produced from the Yb mesh, the lower panels Pt mesh parameters.

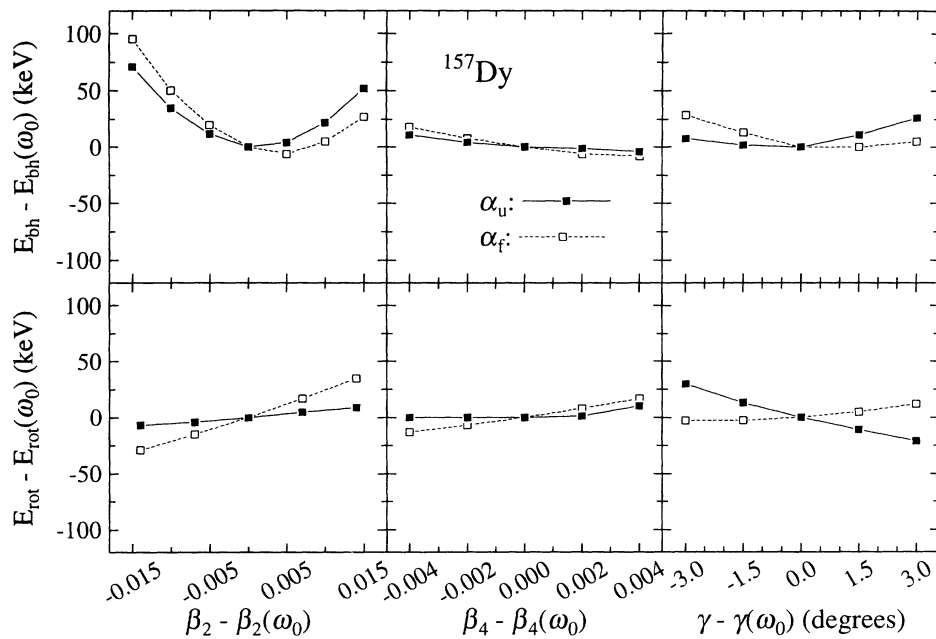


FIG. 7. Calculated Routhian and bandhead energies for ^{157}Dy as functions of variations in β_2 , β_4 , and γ . Deformation parameters $\beta_2(\omega_0)$, $\beta_4(\omega_0)$, and $\gamma(\omega_0)$ were extracted from TRS calculations at $\hbar\omega = 0.2$ MeV. The quantities $E_{bh}(\omega_0)$ and $E_{rot}(\omega_0)$ are the calculated energies at $\hbar\omega_0 = 0.2$ MeV obtained by means of the Strutinsky renormalization procedure and cranking calculations, respectively, using $\beta_2(\omega_0)$, $\beta_4(\omega_0)$, and $\gamma(\omega_0)$.

occur for light Dy, where the calculated signature splitting is as much as 131 keV larger than the measured value (for $N = 89$). There seems to be the trend of increasing deviation for decreasing neutron number. This is not surprising since these systems are deformation soft and, therefore, most susceptible to shape changes as a function of rotation. These deviations are greater than the uncertainties of the calculations, as discussed in the following paragraph.

The experimental uncertainties on $\nu i_{13/2}$ signature splitting are small. It is important, therefore, to estimate the uncertainty in the calculated $\Delta e'$. Even though our calculational method minimizes interpolation uncertainties in TRS, there are still uncertainties in the calculated

deformation parameters, since they are obtained from an interpolation between points of the mesh. For example, uncertainties of ± 0.007 and ± 0.002 , respectively, in the β_2 and β_4 values are quoted Ref. [18] in a bandhead potential energy surface calculation which had a finer step size than the calculation in our analysis. While it is not documented, a conservative estimate for the uncertainty in γ would be $\pm 1.5^\circ$. To test the sensitivity of the calculated $\Delta e'$ to changes in deformation, we repeated calculations using deformation parameters within twice the above uncertainties of the TRS parameters. These calculations were performed for two nuclei, ^{157}Dy and ^{167}Yb , and are summarized in Figs. 7 and 8. The results indicate that variation in β_4 has very little effect on

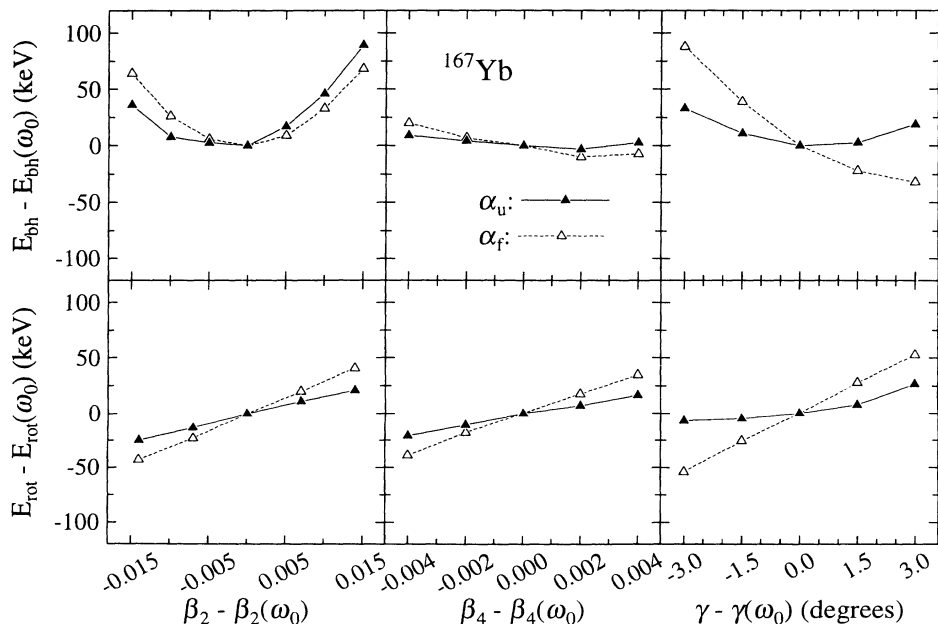


FIG. 8. Calculated Routhian and bandhead energies for ^{167}Yb as functions of variations in β_2 , β_4 , and γ . Deformation parameters $\beta_2(\omega_0)$, $\beta_4(\omega_0)$, and $\gamma(\omega_0)$ were extracted from TRS calculations at $\hbar\omega = 0.2$ MeV. The quantities $E_{bh}(\omega_0)$ and $E_{rot}(\omega_0)$ are the calculated energies at $\hbar\omega_0 = 0.2$ MeV obtained by means of the the Strutinsky renormalization procedure and cranking calculations, respectively, using $\beta_2(\omega_0)$, $\beta_4(\omega_0)$, and $\gamma(\omega_0)$.

the bandhead and rotational energies for both ^{157}Dy and ^{167}Yb . Changing β_2 for both signatures simultaneously results in very little change in total $\Delta e'$. For example, decreasing β_2 by 0.007 for both signatures of ^{157}Dy causes a decrease in ΔE_{def} by approximately 12 keV, and an increase in ΔE_{rot} by 11 keV, which gives a change in total $\Delta e'$ of only -1 keV. Varying β_2 for only a single signature results, of course, in a greater change in $\Delta e'$, although certainly not large. A decrease of 0.007 in β_2 for the favored ($\alpha = \frac{1}{2}$) signature in ^{157}Dy results in a net change of -16 keV to the total $\Delta e'$. Variations in γ likewise have only a small effect on $\Delta e'$, since the changes in ΔE_{def} and ΔE_{rot} are nearly equal and opposite. The exception to this is the unfavored signature ($\alpha = -\frac{1}{2}$) in ^{167}Yb in which both ΔE_{def} and ΔE_{rot} increase as γ increases. A $\Delta\gamma = 3^\circ$ increase in γ for the unfavored signature in ^{167}Yb results in an increase in $\Delta e'$ by 46 keV. This is the largest deviation in $\Delta e'$ by changing a single deformation parameter within the chosen uncertainties in either ^{157}Dy or ^{167}Yb .

The Δ dependence of the results were tested by performing cranking calculations with varying pairing energies. The results of these calculations are presented in Fig. 9, and indicate that for systems with Fermi levels low in the $\nu i_{13/2}$ subshell ΔE_{rot} is not extremely sensitive to pairing changes. Variations of 50 keV in pairing energy produces a maximum change in $\Delta e'$ of 11 keV for ^{167}Yb and 5 keV for ^{157}Dy .

From the results shown in Figs. 7, 8, and 9, it is clear that the discrepancies between the calculated and experimental $\Delta e'$ for the lighter nuclei in this analysis are not due to small errors in deformation or pairing. One source

for the deviations between theory and experiment may be due to coupling of γ -vibrational modes to the $\nu i_{13/2}$ rotational bands. As discussed by Matsuzaki *et al.* [19,20], calculations of $\Delta e'$ with a generalized γ vibration coupling to $\nu i_{13/2}$ bands can lead to reductions of as much as 70 keV in the $\nu i_{13/2}$ signature splitting.

Another contribution to the signature splitting is expected to come from the higher-multipolarity part of the pairing interaction, e.g., quadrupole pairing. As illustrated by Diebel [21] a small change of the quadrupole equilibrium deformation of a one-quasiparticle orbital $|i\rangle$ is expected due to the state dependence of the pairing g_{2P} ,

$$\Delta_i = \Delta_{00} + (Q_{20})_i \Delta_{20} + (Q_{22} + Q_{2-2})_i \Delta_{22}. \quad (5.1)$$

The shift in equilibrium deformation caused by quadrupole pairing can lead to a contribution to the deformation part of the signature splitting, ΔE_{def} . On the other hand, the $K^\pi=1^+$ part of the quadrupole interaction is known to reduce the strength of the Coriolis coupling,

$$-\omega \langle \alpha | j_x | \beta \rangle (u_\alpha u_\beta + v_\alpha v_\beta) \rightarrow -\omega \langle \alpha | j_x | \beta \rangle \times (u_\alpha u_\beta + v_\alpha v_\beta) (1 - P_{\alpha\beta}), \quad (5.2)$$

where the reduction factor $P_{\alpha\beta}$ (usually positive) depends on the position of the Fermi level in the shell (see Ref. [22], Eqs. (12), (34), (35)). Consequently, the $K^\pi=1^+$ component of quadrupole pairing is expected to contribute directly to ΔE_{rot} . In order to make a quantitative statement on the magnitude of both corrections, deformation and pairing self-consistent calculations in-

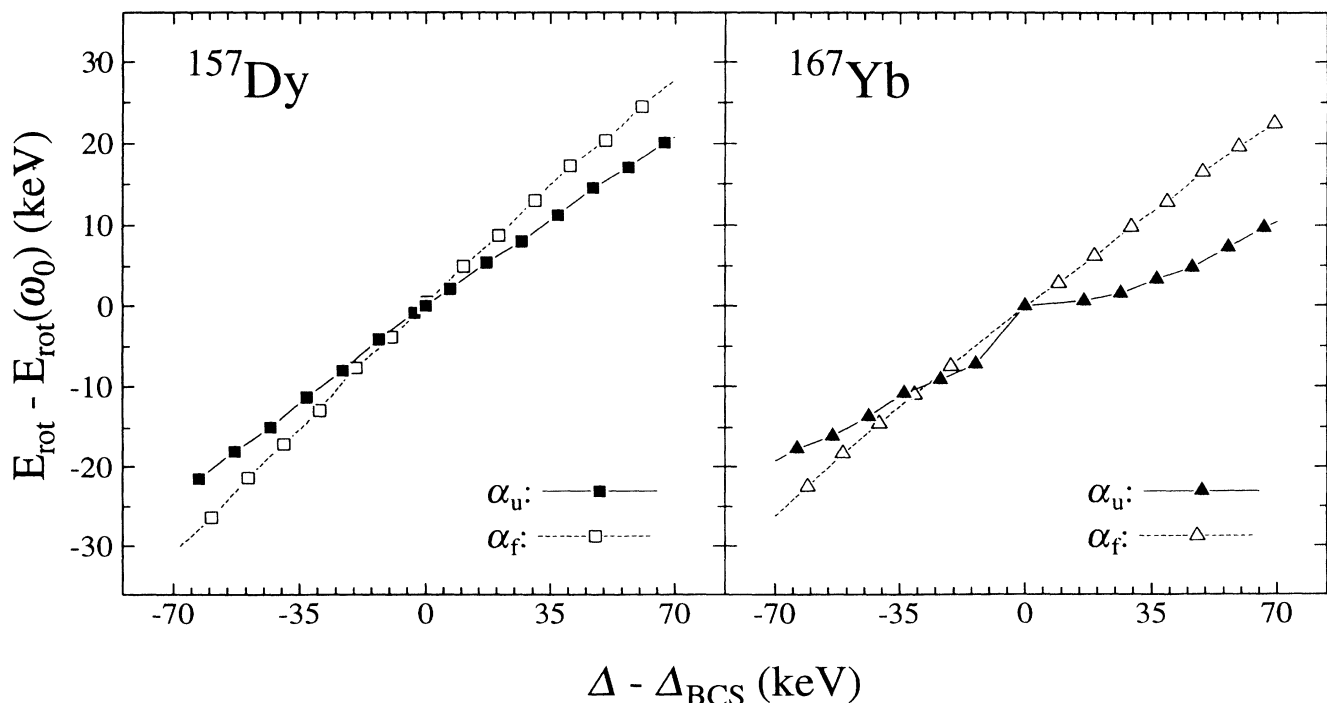


FIG. 9. Calculated Routhian energies for ^{157}Dy and ^{167}Yb as functions of variations in pairing energy. The BCS pairing gap, Δ_{BCS} , was used to compute $E_{\text{rot}}(\omega_0)$ at $\hbar\omega_0 = 0.2$ MeV.

volving monopole and quadrupole pairing interactions, such as those of Ref. [23], are needed.

Other reasons for these deviations in the calculated $\Delta e'$ values include a difference in the overall band-head renormalization due to the zero-point rotational energy [18,24,25], an approximate treatment of rotation (assumption of good quantum number K), the presence of configuration-dependent pairing forces (see, e.g., Refs. [22,26]), and the effect of ω -induced terms in the self-consistent Hamiltonian [27,28].

VI. CONCLUSIONS

The energy splitting between the two signatures of a rotational band based on a high- j orbital is a measurable, regularly varying with N and Z . The experimental trend for the $\nu i_{13/2}$ orbital in $Z = 62 - 78$ nuclei indicates that $\Delta e'$ is as high as 500 keV low in the $i_{13/2}$ shell ($N = 89$) and decreases to 30 - 40 keV at $N = 107$ (when the Fermi level is near the $\Omega = \frac{9}{2}$ orbital). Before proceeding to an analysis of the more complicated trend for $\pi h_{9/2}$ (complex due to the close-lying $h_{11/2}$ orbitals), we apply a detailed theoretical analysis to the $\nu i_{13/2}$ $\Delta e'$ trend. A microscopic calculation is performed in a way in which (a) pairing can be treated self-consistently and (b) deformation and pairing are allowed to be different for each signature. Deformations for this wide range of studied nuclei are extracted from two different TRS meshes, which give a consistent 5% difference in deformation for the overlapping isotopes. However, this difference affects both signatures and thus the variation in calculated $\Delta e'$ is small. The TRS-predicted deformation difference between signatures would have little effect on most measurable quantities but impacts the signature-splitting calculation a great deal. Also, for the cases studied, pairing energy had very little effect on the signature splitting, because for both the self-consistent and the non-self-consistent calculations, the difference in pairing energy between the two signatures was small at $\hbar\omega = 0$. Good agreement is obtained between the experimental

and theoretical results for isotopes of Er, Yb, Hf, W, and Os, with the exceptions of ^{175}W , ^{175}Os , and ^{177}Os . The difference between theory and experiment for these three isotopes is likely due to a slightly improper $N = 102$ gap in the single-particle level energies. Suggested [18] uncertainties in deformation values extracted from TRS mesh calculations are incorporated to test one component of the uncertainties in the final $\Delta e'$ values. We find that the deviations (as large as 131 keV for $N = 89$ Dy) cannot be explained by reasonable uncertainties in extracted deformation or pairing parameters, but instead may be related to effects not included in the model (e.g., dynamic couplings to γ vibrational modes or quadrupole pairing). In spite of these differences for the "softest" nuclei in this survey, it is clear that the agreement between experiment and theory allows one to proceed to the next level of investigation. In the next publication, the trend of signature splitting for $\pi h_{9/2}$ bands in $Z = 69$ to 79 nuclei will be presented and compared to calculations. Such a comparison is important for addressing the often peculiar features of $h_{9/2}$ proton bands. And, our overall goal is to demonstrate that signature splitting is reliable and calculable enough to use as a fingerprint in multi-quasiparticle bands as we proceed to the identification of a greater variety of rotational structures in experiment.

ACKNOWLEDGMENTS

Oak Ridge National Laboratory is managed for the U.S. Department of Energy by Martin Marietta Energy Systems, Inc. under contract No. DE-AC05-84OR21400. The Joint Institute for Heavy Ion Research has as member institutions the University of Tennessee, Vanderbilt University, and the Oak Ridge National Laboratory; it is supported by the members and by the Department of Energy through Contract No. DE-FG05-87ER40361 with the University of Tennessee. Theoretical nuclear physics research at the University of Tennessee is supported by the U.S. Department of Energy through Contract No. DE-FG05-93ER40770.

-
- [1] S. Shastry, J. C. Bacelar, J. D. Garrett, G. B. Hagemann, and B. Herskind, Nucl. Phys. **A470**, 253 (1987).
 - [2] S. Frauendorf and F. R. May, Phys. Lett. **125B**, 245 (1983).
 - [3] I. Hamamoto and B. R. Mottelson, Phys. Lett. **127B**, 281 (1983).
 - [4] R. Bengtsson, W. Nazarewicz, Ö. Skeppstedt, and R. Wyss, Nucl. Phys. **A528**, 215 (1991).
 - [5] W. Nazarewicz, G. A. Leander, and J. Dudek, Nucl. Phys. **A467**, 437 (1987).
 - [6] W. Nazarewicz, R. Wyss, and A. Johnson, Nucl. Phys. **A503**, 285 (1989).
 - [7] R. Wyss, in *Nuclear Structure Models*, edited by R. Bengtsson, J. Draayer, and W. Nazarewicz (World Scientific, Singapore, 1993), p. 196.
 - [8] L. L. Riedinger, J. Avakian, H.-Q. Jin, W. F. Mueller, and C.-H. Yu, Prog. Part. Nucl. Phys. **28**, 75 (1992).
 - [9] L. L. Riedinger, W. F. Mueller, and C.-H. Yu, in *International Conference on Nuclear Structure at High Angular Momentum* (AECL, Ottawa, Canada, 1992), Report No. 10613, Vol. 2, p. 339.
 - [10] L. L. Riedinger, H. J. Jensen, W. F. Mueller, W. Reviol, C.-H. Yu, J.-Y. Zhang, and W. Nazarewicz, in *International Symposium on Nuclear Physics of Our Times*, edited by A. V. Ramayya (World Scientific, Singapore, 1993), p. 239.
 - [11] R. Bengtsson and S. Frauendorf, Nucl. Phys. **A327**, 139 (1979).
 - [12] A. Bohr and B. R. Mottelson, *Nuclear Structure*, Vol. 2 (Benjamin, New York, 1975).

- [13] I. M. Pavlichenkov, *Phys. Rep.* **226**, 173 (1993).
- [14] R. Wyss and J. Nyberg, private communication.
- [15] W. Nazarewicz, J. Dudek, R. Bengtsson, T. Bengtsson, and I. Ragnarsson, *Nucl. Phys.* **A435**, 397 (1985).
- [16] R. Wyss, W. Satuła, W. Nazarewicz, and A. Johnson, *Nucl. Phys.* **A511**, 324 (1990).
- [17] I. Hamamoto, *Nucl. Phys.* **A271**, 15 (1976).
- [18] W. Nazarewicz, M. A. Riley, and J. D. Garrett, *Nucl. Phys.* **A512**, 61 (1990).
- [19] M. Matsuzaki, Y. R. Shimizu, and K. Matsuyanagi, *Prog. Theor. Phys.* **79**, 836 (1988).
- [20] M. Matsuzaki, *Nucl. Phys.* **A491**, 433 (1989).
- [21] M. Diebel, *Nucl. Phys.* **A419**, 221 (1984).
- [22] I. Hamamoto, *Nucl. Phys.* **A232**, 445 (1974).
- [23] W. Satuła and R. Wyss, *Phys. Rev. C* (submitted).
- [24] M. E. Bunker and C. W. Reich, *Rev. Mod. Phys.* **43**, 348 (1971).
- [25] W. Ogle, S. Wahlborn, R. Piepenbrink, and S. Fredriksson, *Rev. Mod. Phys.* **43**, 424 (1971).
- [26] I. Hamamoto and W. Nazarewicz, *Phys. Rev. C* **99** 2489 (1994).
- [27] Y. M. Engel, D. M. Brink, K. Goeke, S. J. Krieger, and D. Vautherin, *Nucl. Phys.* **A249**, 215 (1975).
- [28] B.-Q. Chen, P.-H. Heenen, P. Bonche, M. S. Weiss, and H. Flocard, *Phys. Rev. C* **46**, R1582 (1992).
- [29] M. A. Riley, N. J. Ward, P. D. Forsyth, H. W. Griffiths, D. Howe, J. F. Sharpy-Schafer, J. Simpson, J. C. Lisle, E. Paul, and P. Walker, *Proceedings from the 5th Nordic Meeting on Nuclear Physics, Jyväskylä, Finland, 1984*.
- [30] B. Singh, J. A. Szücs, M. W. Johns, *Nuclear Data Sheets* **55**, 185 (1988).
- [31] M. A. Lee, *Nuclear Data Sheets* **37**, 487 (1982).
- [32] R. G. Helmer, *Nuclear Data Sheets* **55**, 88 (1988).
- [33] M. A. Deleplanque, J. C. Bacelar, E. M. Beck, R. M. Diamond, J. E. Draper, R. J. McDonald, and F. S. Stephens, *Phys. Lett. B* **193**, 422 (1987).
- [34] J. J. Gaardhøje, PhD. thesis, University of Copenhagen, 1980; L. L. Riedinger, *Nucl. Phys.* **A347**, 141 (1980).
- [35] M. A. Lee, *Nuclear Data Sheets* **53**, 521 (1988).
- [36] J. D. Garrett, G. B. Hagemann, B. Herskind, J. Bacelar, R. Chapman, J. C. Lisle, J. N. Mo, A. Simcock, J. C. Willmott, and H. G. Price, *Phys. Lett.* **118B**, 297 (1982).
- [37] J. Kownacki, J. D. Garrett, J. J. Gaardhøje, G. B. Hagemann, B. Herskind, S. Jónsson, N. Roy, H. Ryde, and W. Walús, *Nucl. Phys.* **A464**, 472 (1987).
- [38] L. K. Peker, *Nuclear Data Sheets* **50**, 137 (1987).
- [39] M. Oshima, E. Minehara, S. Ichikawa, H. Imura, T. Inamura, A. Hashizume, H. Kushakari, and S. Iwasaki, *Phys. Rev. C* **37**, 2578 (1988).
- [40] J. C. Bacelar, M. Diebel, O. Andersen, J. D. Garrett, G. B. Hagemann, B. Herskind, L. Carlén, J. Lyttkens, H. Ryde, W. Walús, and P. O. Tjøm, *Phys. Lett.* **152B**, 157 (1985).
- [41] E. M. Beck, J. C. Bacelar, M. A. Deleplanque, R. M. Diamond, F. S. Stephens, J. E. Draper, B. Herskind, A. Holm, and P. O. Tjøm, *Nucl. Phys.* **A464**, 472 (1987).
- [42] V. S. Shirley, *Nuclear Data Sheets* **58**, 974 (1989).
- [43] J. C. Bacelar, M. Diebel, C. Ellegaard, J. D. Garrett, G. B. Hagemann, B. Herskind, A. Holm, C.-X. Yang, J.-Y. Zhang, P. O. Tjøm, and J. C. Lisle, *Nucl. Phys.* **A442**, 509 (1985).
- [44] M. A. Lee, *Nuclear Data Sheets* **53**, 223 (1988).
- [45] J. Espino, J. D. Garrett, G. B. Hagemann, P. O. Tjøm, C.-H. Yu, M. Bergström, L. Carlén, L. P. Ekström, J. Lyttkens-Lindén, H. Ryde, R. Bengtsson, T. Bengtsson, R. Chapman, D. Clarke, F. Khazaie, J. C. Lisle, and J. N. Mo, *Nucl. Phys.* **A567**, 377 (1994).
- [46] R. A. Bark, G. D. Dracoulis, and A. E. Stuchbery, *Nucl. Phys.* **A514**, 503 (1990).
- [47] B. Cederwall, R. Wyss, A. Johnson, J. Nyberg, B. Fant, R. Chapman, D. Clark, F. Khazaie, J. C. Lisle, J. N. Mo, J. Simpson, and I. Thorlund, *Z. Phys. A* **337**, 283 (1990).
- [48] V. S. Shirley, *Nuclear Data Sheets* **43**, 162 (1984).
- [49] P. M. Walker, G. D. Dracoulis, A. Johnston, J. R. Leigh, M. G. Slocombe, and I. F. Wright, *J. Phys. G* **4**, 1655 (1978).
- [50] B. Fabricius, G. D. Dracoulis, R. A. Bark, A. E. Stuchbery, T. Kibedi, and A. M. Baxter, *Nucl. Phys.* **A511**, 345 (1990).
- [51] G. D. Dracoulis, B. Fabricius, R. A. Bark, A. E. Stuchbery, D. G. Popescu, and T. Kibedi, *Nucl. Phys.* **A510**, 533 (1990).
- [52] V. S. Shirley, *Nuclear Data Sheets* **43**, 127 (1984).
- [53] V. S. Shirley, *Nuclear Data Sheets* **54**, 589 (1988).
- [54] G. D. Dracoulis, C. Fahlander, and A. P. Byrne, *Nucl. Phys.* **A401**, 490 (1983).
- [55] A. Djaffri, Ph.D. thesis, University of Montreal, 1991.
- [56] M. M. Minor, *Nuclear Data Sheets* **18**, 331 (1976).
- [57] M. J. A. de Voigt, R. Kaczarowski, H. J. Riezobos, R. F. Noorman, J. C. Bacelar, M. A. Deleplanque, R. M. Diamond, and F. S. Stephens, *Nucl. Phys.* **A507**, 447 (1990).
- [58] P. M. Walker, G. D. Dracoulis, A. P. Byrne, B. Fabricius, T. Kibédi, and A. E. Stuckbery, *Phys. Rev. Lett.* **67**, 433 (1991).
- [59] A. Neskakis, R. M. Lieder, M. Müller-Veggian, H. Beuscher, W. F. Davidson, and C. Mayer-Böricke, *Nucl. Phys.* **A261**, 189 (1976).
- [60] J. Nyberg, A. Johnson, M. P. Carpenter, C. R. Bingham, L. H. Courtney, V. P. Janzen, S. Juutinen, A. J. Larabee, Z.-M. Liu, L. L. Riedinger, C. Baktash, M. L. Halbert, N. R. Johnson, I. Y. Lee, Y. Schutz, J. C. Waddington, and D. G. Popescu, *Nucl. Phys.* **A511**, 92 (1990).
- [61] F. Hannachi, G. Bastin, M. G. Porquet, J. P. Thibaud, C. Bourgeois, L. Hildingsson, N. Perrin, H. Sergolle, F. A. Beck, and J. C. Merdinger, *Z. Phys. A* **330**, 15 (1988).
- [62] R. B. Firestone, *Nuclear Data Sheets* **43**, 289 (1984).
- [63] S. Pilotte, G. Kajrys, S. Monaro, M. P. Carpenter, V. P. Janzen, L. L. Riedinger, J. K. Johansson, D. G. Popescu, D. D. Rajnauth, and J. C. Waddington, *Phys. Rev. C* **40**, 610 (1989).
- [64] F. Hannachi, G. Bastin, M. G. Porquet, C. Schück, J. P. Thibaud, C. Bourgeois, L. Hildingsson, D. Jerrestam, N. Perrin, H. Sergolle, F. A. Beck, T. Byrski, J. C. Merdinger, and J. Dudek, *Nucl. Phys.* **A481**, 135 (1988).